Molecular Crystals and Liquid Crystals

ISSN: 1542-1406 (Print) 1563-5287 (Online) Journal homepage: http://www.tandfonline.com/loi/gmcl20

Chiral Dopants Derived from Ephedrine/Pseudoephedrine: Structure and Medium Effects on the Helical Twisting Power

Monika Bauer, Lutz Hartmann, Erich Kleinpeter, Frank Kuschel, Cornelia Pithart & Wolfgang Weissflog

To cite this article: Monika Bauer, Lutz Hartmann, Erich Kleinpeter, Frank Kuschel, Cornelia Pithart & Wolfgang Weissflog (2015) Chiral Dopants Derived from Ephedrine/Pseudoephedrine: Structure and Medium Effects on the Helical Twisting Power, Molecular Crystals and Liquid Crystals, 608:1, 14-24, DOI: 10.1080/15421406.2014.949592

To link to this article: http://dx.doi.org/10.1080/15421406.2014.949592

Published online: 03 Mar 2015.

Mol. Cryst. Liq. Cryst., Vol. 608: pp. 14–24, 2015

ISSN: 1542-1406 print/1563-5287 online
DOI: 10.1080/15421406.2014.949592

Chiral Dopants Derived from Ephedrine/Pseudoephedrine: Structure and Medium Effects on the Helical Twisting Power

MONIKA BAUER,[1] LUTZ HARTMANN,[1,*]
ERICH KLEINPETER,[2] FRANK KUSCHEL,[1]
CORNELIA PITHART,[1] AND WOLFGANG WEISSFLOG[3]

[1]Fraunhofer Research Institution for Polymeric Materials and Composites PYCO, Teltow, Germany
[2]Department of Chemistry, University of Potsdam, Potsdam, Germany
[3]Institute of Physical Chemistry, Martin-Luther-University Halle-Wittenberg, Halle, Germany

Chiral dopants were obtained by acylation of enantiomerically pure ephedrine and pseudoephedrine with promesogenic carbonyl reagents. The products have been investigated with respect to their chiral transfer ability on nematic host matrices characterized by extreme differences of the dielectric anisotropy. It has been found that the medium dependence of the helicity induction nearly disappears at reduced temperatures. Based on variable temperature ^1H NMR studies on monoacylated homologues, the estimated coalescence temperatures and free activation enthalpies for the hindered rotation around C—N bonds could be correlated with the helical twisting power. Measurements by dielectric spectroscopy reveal the correlation between the molar mass of substituents linked to the chiral building block and the dynamic glass transition of corresponding chiral dopants. Furthermore, the effect of intramolecular and intermolecular hydrogen bonds has been studied by ATR-FTIR spectroscopy.

Keywords Chiral dopants; ephedrine/pseudoephedrine; molecular structure; ^1H NMR; dielectric spectroscopy; ATR-FTIR

1. Introduction

The transfer of chirality by chiral dopants to achiral nematics is a proper method for preparation of cholesteric and ferroelectric LC material. Apart from the classical cholesterol ester, there is a huge number of appropriate compounds, such as derivatives of carbohydrates [1], 1,2-ethandiol [2], tartaric acid [3], bi-2-naphthol [4], helicene [5], or more recently phenyl-ethylamine alkaloids [6]. In comparison to the use of a single mesogenic substance with inherent chirality, mixtures prepared by doping offer considerably more possibilities to tune the materials properties (helical structure, phase range, optic and dielectric key figures). Hence it is possible to realize numerous highly interesting technical applications,

*Address correspondence to Lutz Hartmann, Fraunhofer Research Institution for Polymeric Materials and Composites PYCO, Kantstr. 55, D-14513 Teltow, Germany. E-mail: lutz.hartmann@pyco.fraunhofer.de

for example, thermal imagers, radiation detectors, optical filters, light modulators, coloring effect materials [7] or bistable displays [8].

An important dopant parameter characterizing the ability to induce a helical structure is the helical twisting power, $HTP_x = (dp^{-1}/dx)_{x=0} \approx 1/(px)$, where p is the pitch length of the helix and x is the dopant molar fraction. Generally, an ideal dopant applicable in devices should comprise a high HTP_x, a sufficient solubility in the host medium and photostability. Application tests revealed that only a small fraction of the dopants suggested in the literature is suited for the application under stringent conditions [9]. However, beyond practical aspects, the design of dopants with special properties implies the understanding of the structure-activity-relationships. Generally, the chirality transfer should be controlled by the dopant-host interaction and the order parameter of the LC matrix [10]. Different model approaches for the prediction of the twisting ability have been applied and the results were compared with experimentally measured HTP values [10, 11]. But reliable structure-property correlations could only be found within dopant classes of similar molecular structures [12, 13]. Anyway, such studies could be essential building blocks for a generally valuable perception allowing the preparation of tailor-made chiral mesogenic phases.

In continuation of our studies on dopants derived from 1-phenyl-2-aminoalcohols bearing two stereogenic centers, especially enantiomerically pure ephedrine and pseudoephedrine, we studied structure-property relationships in terms of chirality transfer on selected host systems. To this end, we used homologous mono- and diacylated stereoisomers with an uniform substitution pattern and two nematic hosts of extremely different composition and polarity. In detail, the HTP_x and its temperature and host medium dependence have been measured. Furthermore, it is well investigated that certain stereoisomers exhibit significantly different biological activity [14]. This concerns especially atropisomers consisting of relatively slow interconverting conformers characterized by a half life of more than 1000 s. Such conformers may be formed by hindered rotation along a —N—CO— bond due to neighboring space demanding substituents or electronic effects. Of course, depending on the height of the rotational barrier, geometrical isomers with higher exchange rate may be observed (rotamers). The —N—CO— bond in the above mentioned N-acylated dopants exhibits a partial double-bond character. Therefore, the existence of rotamers could be expected. Aside the prove of exchanging rotamers by NMR, it was of interest to learn if there are consequences with respect to the chiral transfer activity. For this reason, variable temperature ^{1}H NMR studies were carried out. Dielectric spectroscopy has been employed to investigate the impact of various substituents on the relaxation time of the dynamic glass transition (α-relaxation) and its temperature dependence. A part of the substances formed hydrogen bonds. Therefore, temperature-dependent IR spectra have been recorded.

2. Experimental Procedure

2.1. Materials

The chemical structure and synthesis of the substituted chiral 1-phenyl-2-amino-alcohols have been described previously [6]. Coming from the structure of the central chiral unit (Fig. 1) and the substituents (Fig. 2), the investigated substances together with the configuration of the initial aminoalcohols are summarized in Table 1.

R^1 and R^2 represent the substituents **Cy** and **Np** explained in Fig. 2. In case of the monoacylated compounds, R^2 denotes H.

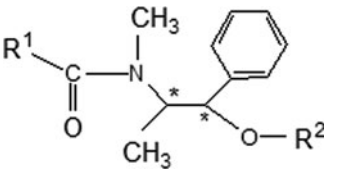

Figure 1. Structure of the chiral building block.

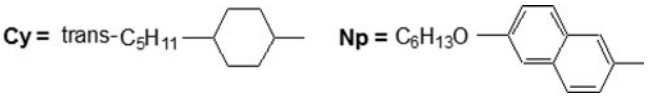

Figure 2. The substituents **Cy** and **Np.**

For comparison, the commonly used chiral dopant **CB15** ((S)-4-cyano-4′-(2-methylbutyl)biphenyl, Merck KGaA) has been involved in our measurements. As host systems, two differing nematic matrices have been selected: The multi-component mixture **MLC-6650** (Merck KGaA) and the single component trans-4-*n*-butylcyclohexancarboxylic acid 4′-*n*-hexyloxyphenylester (**BCHOP**) [15]. As it is apparent from Table 2, both systems differ significantly with respect to their thermal, optical and dielectric behavior.

2.2. Methods

To measure HTP_x, the screw sense of the helix and the temperature dependence, solutions containing about 1 wt% of the dopant in the respective host were prepared and filled in wedged glass cells (E.H.C./Tokyo). The cells were analyzed using a polarizing microscope equipped with a hot stage and a temperature controller.

For routine structure analyses, ^1H and ^{13}C NMR spectra at room temperature were recorded on an Agilent 500 MHz spectrometer with $CDCl_3$ as solvent.

Table 1. Constituents and melting points of mono- and diacylated ephedrine (**E**) or pseudoephedrine (**PE**) (cf. Figs. 1 and 2). A denotes the configuration of the starting aminoalcohol

Code	R^1	A	R^2	M_p / °C
E-1Cy	Cy	(1R,2S)-(-)	H	77–79
E-2Cy	Cy	(1R,2S)-(-)	-OC-Cy	85–87
E-1Np	Np	(1R,2S)-(-)	H	89–90
E-2Np	Np	(1R,2S)-(-)	-OC-Np	128–130
PE-1Cy	Cy	(1S,2S)-(+)	H	91–93
PE-2Cy	Cy	(1S,2S)-(+)	-OC-Cy	69–71
PE-1Np	Np	(1S,2S)-(+)	H	143–145
PE-2Np	Np	(1S,2S)-(+)	-OC-Np	glass

Table 2. Properties of the host systems (Cr – crystalline, S_G – smectic G, N – nematic, Is – isotropic, Δn – birefringence, $\Delta\varepsilon$ – dielectric anisotropy)

Code	Thermal properties/°C	$\Delta\varepsilon$ (20°C)	Δn (20°C)	Lit.
MLC-6650	−40 N 90 Is	52.6	0.1537	[16]
BCHOP	Cr 25 (S_G 22) N 70 Is	≈ -1	0.077	[17, 18]

Variable temperature ^{1}H NMR studies of **E-1Cy**, **E-1Np**, **PE-1Cy**, and **PE-1Np** between 298 K and 373 K were performed on a Bruker AVANCE III spectrometer at 600.24 MHz in DMSO-d_6.

Spectra of the dielectric loss ε'' in a frequency range between 10^7 Hz and 5×10^{-2} Hz and at temperatures between 385 K and 260 K with an increment of 5 K were recorded on a Concept 80 System by Novocontrol. Sample capacitors were prepared by melting the dopants on a brass electrode with a diameter of 10 mm. The second electrode was separated by glass fiber spacers (diameter 50 μm) placed into the molten dopants.

The FTIR spectra were collected using a Nicolet 5700 FTIR spectrometer equipped with an ATR-unit (Thermo Fisher Scientific Inc.).

3. Results and Discussion

The HTP_x values of the compounds listed in Table 1 were measured between ambient and isotropization temperatures. The results are illustrated in Fig. 3. To facilitate the visual clarity of the data, absolute values of HTP_x are presented.

For an independent comparison between the dopants and with respect to molecular structures and interactions, it should be reasonable to use HTP_x data relating to a reduced absolute temperature T_r. Therefore, in Table 3 are listed real HTP_x data for $T_r = 0.97T_i$ with T_i as the nematic-isotropic transition temperature of the host in K.

Figure 3 and Table 3 reveal: (i) After monoacylation at the N atom the replacement of **E** by **PE** causes mostly a decrease of HTP_x. (ii) The introduction of a second acyl moiety by esterification of the OH group gives rise to a drastic increase of the twisting power; in case of **PE** attended by the change of the helix handedness. (iii) Within the group of disubstituted compounds, an increase of HTP_x and a handedness inversion by substitution

Table 3. HTP_x data in μm^{-1} obtained by interpolation to ϑ_r(**MLC-6650**) = T_r(**MLC-6650**) − 273 K = 79°C and ϑ_r(**BCHOP**) = T_r(**BCHOP**) − 273 K = 60°C

Code	MLC-6650	BCHOP
E-1Cy	−6.2	−5.9
E-2Cy	−23	−18
PE-1Cy	−4.4	−4
PE-2Cy	+38	+37
E-1Np	−11	−9
E-2Np	−32	−32
PE-1Np	−7.2	−13
PE-2Np	+47	+72
CB15	+4.3	+4.8

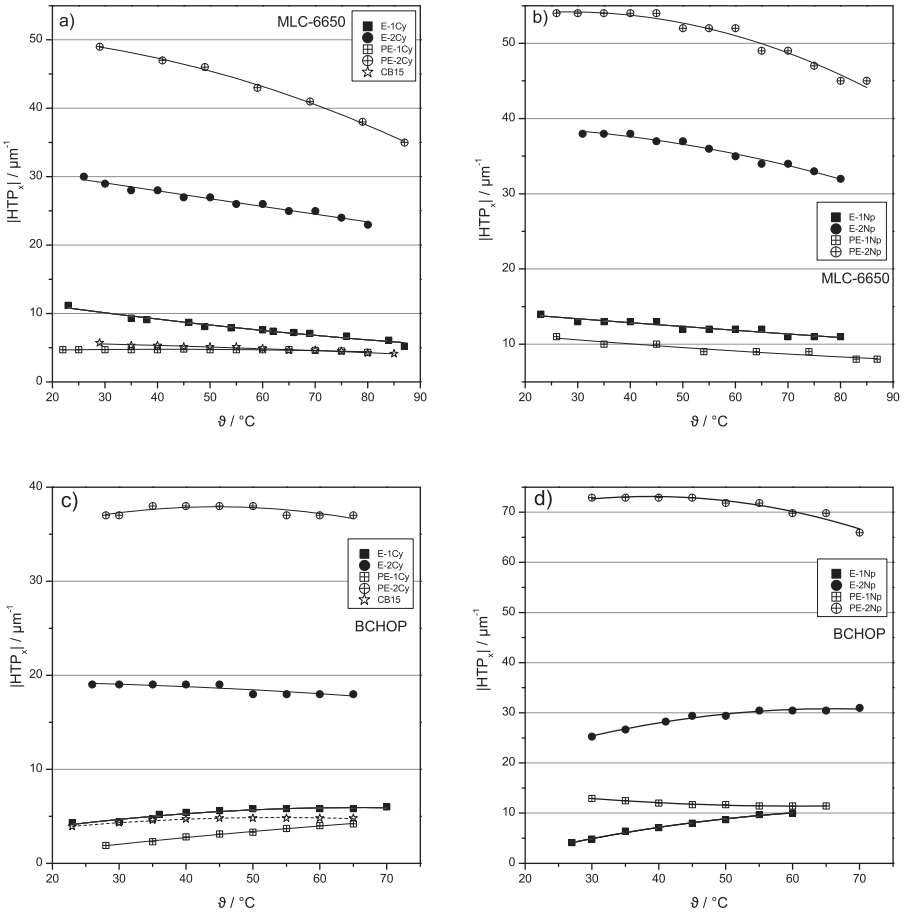

Figure 3. Absolute HTP_x values of dopants listed in Table 1 and of **CB15** in the nematic matrices **MLC-6650** (a, b) and **BCNOP** (c, d). To improve the overview, 2nd order polynomials were fitted to the measured data.

of **E** by **PE** are also observed. (iv) Generally, the temperature dependence of HTP_x is more pronounced for **MLC-6650** solutions than for those prepared from **BCHOP**. (v) Apart from **PE-1Np** and **PE-2Np,** the comparison of the induction ability shows that the host dependence has nearly vanished at reduced temperatures ϑ_r. This circumstance facilitates the disclosing of molecular structure-property relationships for the dopants.

The rotation hindrance about the C—N partial double bond in amides as an example of non-mutual chemical exchange is known for a long time. Especially intramolecular mobility of the amide rotamers characterized by activation energies of 20–100 kJ/mol has been studied by NMR spectroscopy which allows for the analysis of the signal splitting observable at low isomerization rates [19, 20]. In our case the question arose if there are interconnections between conformational dynamics and twisting power. Therefore, variable temperature ^{1}H NMR spectra chemical shift studies with the acylamides **E-1Cy**, **PE-1Cy**, **E-1Np**, and **PE-1Np** have been carried out. For example, Fig. 4 shows the temperature effect on the conformational exchange of **PE-1Cy**. Here, the range and distances of conjugated resonances at 298 K are as follows: $\delta \sim 2.8$ ($\Delta\nu = 43$ Hz, NCH_3), $\delta \sim 3.9$ ($\Delta\nu = 14$ Hz,

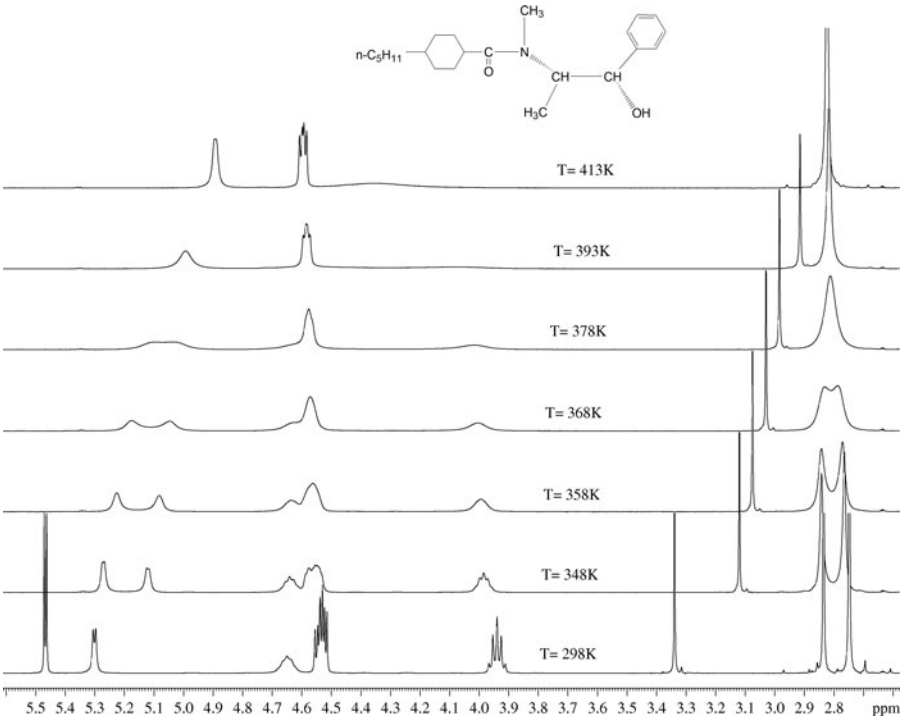

Figure 4. Temperature dependence of the conformational isomerism of **PE-1Cy** in DMSO-d_6. Only the 5.5–2.6 ppm range is presented for a better overview.

C*H*CH$_3$), $\delta \sim 4.6$ ($\Delta\nu = 70$ Hz, C*H*OH). The remarkable δ variation of the low field signals at ca. 5.4 ppm ($\Delta\nu = 83$ Hz, CHO*H*) should be predominantly controlled by hydrogen bonds with the solvent DMSO-d_6. With increasing temperature, the rate of interconversion accelerates and at the coalescence temperature T_c the local minimum between conjugated peaks disappears.

As Fig. 4 reveals, for the rotation about the C—N partial double bond we observed unequal populations of the exchange sites indicating different lifetimes of the species. Therefore, we made use of a method for obtaining the free enthalpy of activation $\Delta G^{\ddagger}$ from T_c and $\Delta\nu$ in case of unequal doublets [21]. The results are summarized in Table 4. Usually, $\Delta G^{\ddagger}$ increases with the spatial extension of the substituents [19].

Table 4. Line separation $\Delta\nu$, coalescence temperature T_c, and free enthalpy of activation $\Delta G^{\ddagger}$ of the monoacylated aminoalcohols. T_c and $\Delta G^{\ddagger}$ represent mean values involving three splitted *H* atom resonances (cf. Fig. 4)

Code	$\Delta\nu$ / Hz [NC*H*$_3$]	T_c / K	$\Delta G^{\ddagger}$ / kJmol^{-1}
E-1Cy	45	376	80
PE-1Cy	43	375	79
E-1Np	95	327	67
PE-1Np	86	338	70

In the actual case, the lowering of the steric rotational hindrance after substitution of **Cy** by **Np** is due to the stabilization of the transition state by conjugation. A similar effect is well known for aromatically substituted dimethylformamide [19, 22]. Certainly, the higher structural flexibility of the **Np** substituted dopants should be an essential contribution to their enhanced twisting power (cf. Table 3.).

Spectra of the dielectric loss ε'' at 328 K for the monoacylated dopants **E-1Cy, PE-1Cy, E-1Np** and **PE-1Np** are shown in Fig. 5(a). Solid lines denote fits of a superposition of a conductivity contribution describing the low frequency dependence of ε'' and the model function by Havriliak and Negami [23] describing the peak in ε'' at higher frequencies. These fits provide a relaxation time $\tau_{\max}$ derived from the maximum position of the relaxation peak whose temperature dependence is shown in Fig. 5(b). For all dopants it can readily be described by the Vogel-Fulcher-Tammann (VFT) equation [24] $\log \tau_{\max} = \log \tau_0 + \frac{B}{T-T_0}$ proving that the relaxation can be assigned to the dynamic glass transition (α-relaxation). τ_0 represents the high temperature limit of the dielectric relaxation time, T_0 is the Vogel temperature and B is a constant. Solid lines in Fig. 5(b) denote fits of the VFT equation to the temperature dependence of $-\log \tau_{\max}$; the fit parameters are given in Table 5.

Obviously, the molecular dipoles contributing to the α-relaxation are mainly localized in the chiral building block (cf. Fig. 1). Furthermore, the different molar masses of the two substituents **Cy** and **Np** has to be considered: While **Cy** has a molar mass of 153 g mol^{-1}, it is about 1.5 times higher for **Ny** with 227 g mol^{-1}. Hence, attaching the heavier and bulkier substituent **Np** to the chiral building blocks leads to the higher dielectric relaxation times compared to **Cy** as revealed in Fig. 5(b).

For a more quantitative discussion we consult the free volume theory which has been developed to justify theoretically the empirical VFT-dependence [25, 26]. It delivers relations connecting the VFT fit parameters to microscopic quantities according to $B = \frac{f^*}{a_f}$ and $T_0 = T_g - \frac{f_g}{a_f}$. Here, f^* is the relative minimal free volume required for a jump of a molecule between two sites, f_g is the relative free volume at the glass transition temperature T_g as indicated in Table 5 and α_f denotes the coefficient of thermal expansion of the free volume. If we assume α_f to be independent on specific molecular structures, we can conclude from the VFT fit parameters that both, f^* and f_g are for **Np** considerably higher than for **Cy**. This is again consistent with the bulkier structure of **Np** compared to that of **Cy**.

Further information has been obtained by ATR-FTIR studies of the neat compounds, especially with respect to the effect of molecular structures and hydrogen bonds on HTP$_x$. Essential results are illustrated in Fig. 6. Generally, all compounds were investigated from

Table 5. Parameters of fits according to the VFT equation in Fig. 5 (b): High temperature limit log τ_0 of dielectric relaxation time, constant B and Vogel temperature T_0. The glass transition temperature T_g is determined by extrapolating the VFT fits to $\tau_{\max} = 100$ s

Code	log τ_0	B / K	T_0 / K	T_g / K
E-1Cy	12.9	769	211	263
PE-1Cy	13.2	781	214	265
E-1Np	12.6	873	229	289
PE-1Np	12.2	826	241	299

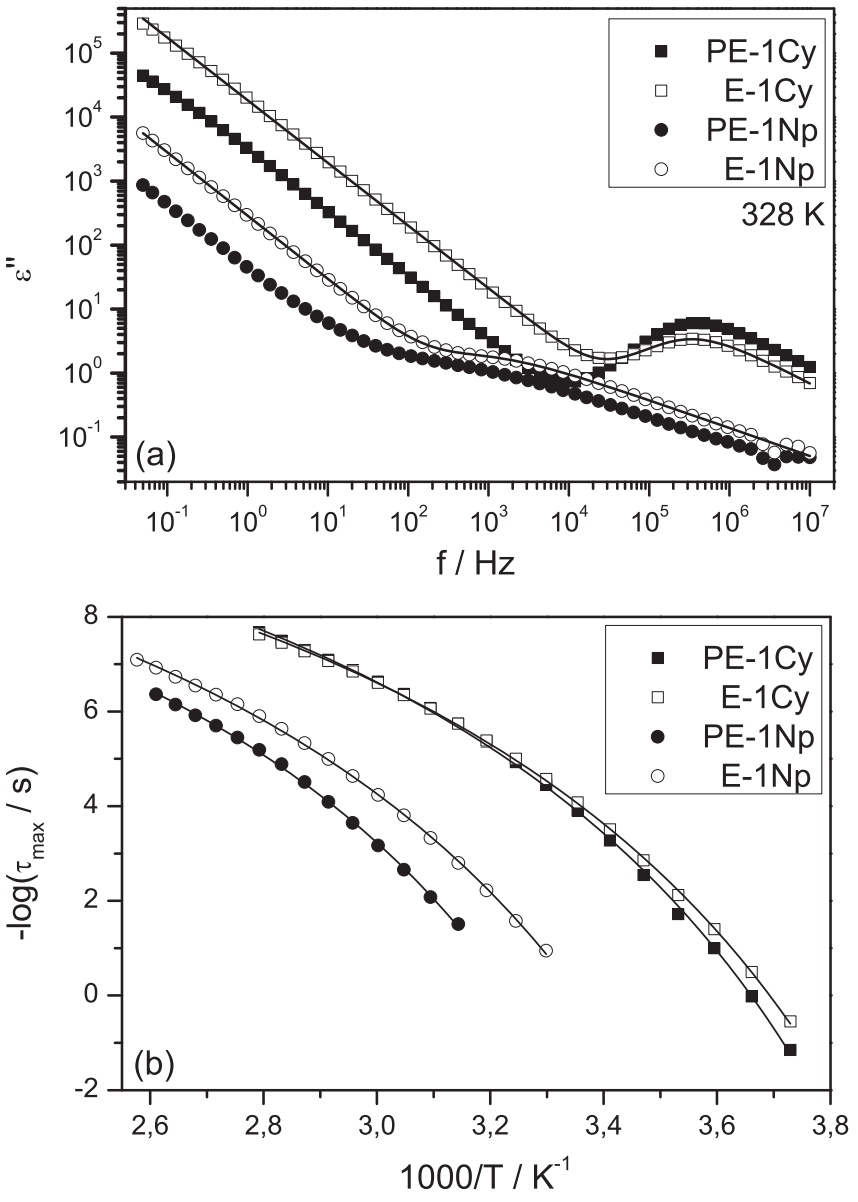

Figure 5. (a) Spectra of dielectric loss ε at 328 K with exemplary fits of the model function by Havriliak and Negami and a conductivity contribution to the data (solid lines). (b) Activation plot for the dielectric relaxation time τ_{max} of the dopants' α-relaxation and fits according to the VFT equation (solid lines).

room temperature up to 80°C, but band positions and shapes were not altered significantly by temperature variation. However, there is a distinct influence of the molecular structure on IR transmission in the region above 3000 cm^{-1}. **E-1Cy** and **PE-1Cy** show narrow IR peaks at 3370 cm^{-1} and 3392 cm^{-1}, whereas relatively broad and flat bands appear in said spectral region for **E-1Np** and **PE-1Np**, respectively. This disparity should be due to the different ratio of intramolecular and intermolecular hydrogen

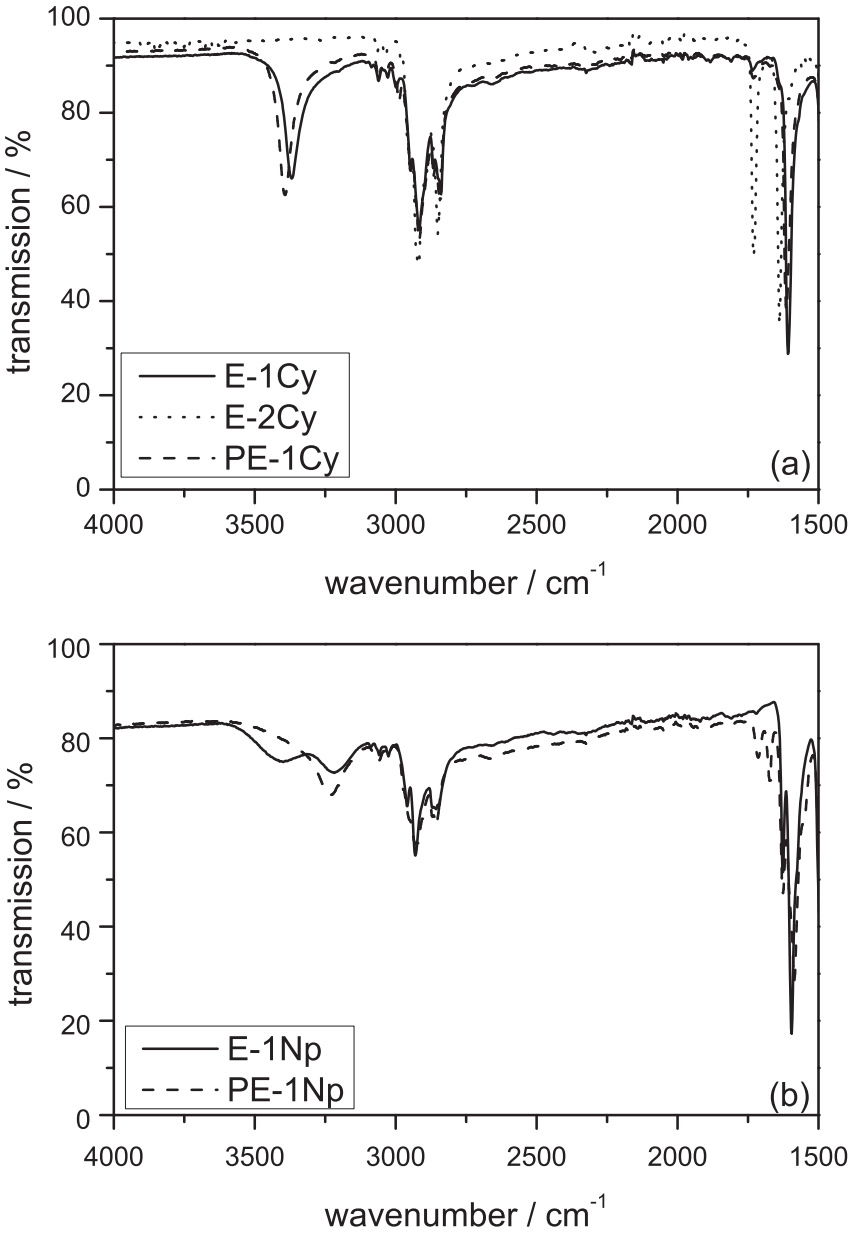

Figure 6. ATR-FTIR spectra of (a) **E-1Cy**, **E-2Cy** and **PE-1Cy** and (b) **E-1Np** and **PE-1Np** at room temperature. For better overview, the graphic representation of the spectra has been limited to the wavenumber region between 4000 cm^{-1} and 1500 cm^{-1}.

bonds. We believe that the twisting capability of the monoacylated dopants is impaired by intramolecular H bridges, as the molecules are interlocked ("frustrated" conformation). Indeed, with decreasing share of intramolecular hydrogen bonding in favor of intermolecular O—H bonds, indicated by the depletion of the O—H stretching frequencies above 3300 cm^{-1}, we found lower free enthalpies of activation (cf. Table 4) as well as higher HTP_x data (cf. Table 3). Regarding the intramolecular flexibility of dopants,

similar conclusions have been drawn from studies about the position of the stereogenic center in relation to the whole molecule [27]. The substitution of trans-n-pentylcyclohexylcarbonyl (**E-1Cy, PE-1Cy)** by 6-*n*-hexyloxynaphthylcarbonyl (**E-1Np**, **PE-1Np)** as N substituents should cause an attenuation of the H bridges as the result from the +M electronic resonance effect of the aromatic rings. Finally, the experimentally proved absence of any hydrogen bonds in the disubstituted compounds **E-2Cy** (exemplarily shown in Fig. 5(a)), **PE-2Cy**, **E-2Np** and **PE-2Np** may be regarded as an essential reason for their much higher twisting power (cf. Table 3).

4. Conclusions

As shown in previous investigations, 1-phenyl-2-aminoalcohols in the form of enantiomerically pure ephedrine and pseudoephedrine and derivatized by gradual acetylation with promesogenic substituents, have been proved as efficient chiral dopants. In this paper is reported on the structure and medium influence of their chirality transfer ability after addition to selected nematic phases. A systematic dependence of the helicity induction from the configuration of the chiral center as well as from the extent of substitution has been found. Measurements of the helical twisting power as a function of temperature revealed that the effect of highly different nematic hosts is minimized at reduced temperatures. As a peculiarity of these dopants, the existence of rotamers due to the hindered rotation around the amide bonds has been proved by variable temperature ^{1}H MNR studies on the monoacylated homologues. Obviously, there is a correlation between the observed coalescence temperatures and activation enthalpies with the twisting power. The differences between the both substituents **Np** and **Cy** with respect to their molar mass and volume manifest in different molecular mobility of monoacylated dopants as revealed by dielectric spectroscopy. According to ATR-FTIR studies, monoacylated homologues are able to form hydrogen bonds whose type depends on the structure of the substituent at the amide position. Because of the much higher HTP data of the diacylated homologues, it is reasoned that the formation of H bonds impairs the functionality as chiral dopants due to restricted molecular flexibility.

Funding

Financial support by the German Federal Ministry of Economics and Technology within the aeronautical research project “INGA - Innovative Galley” (20K1103D) is highly acknowledged.

References

[1] Vill, V., Fischer, F., & Thiem, J. (1988). *Z. Naturforsch. 43a*, 1119.
[2] Heppke, G., Lötzsch, D., & Oestreicher, F. (1986). *Z. Naturforsch.*, *41a*, 1214.
[3] Kuball, H.-G., Weiß, B., Beck, A. K., & Seebach, D. (1997). *Helv. Chim. Acta*, *80*, 2507.
[4] Gottarelli, G., Hibert, M., Samori, B., Solladié, G., Spada, G. P., & Zimmermann, R. (1983). *J. Am. Chem. Soc. 105*, 7318.
[5] Ferrarini, A., Pieraccini, S., Masiero, S., & Spada, G. P. (2009). *Beilstein J. Org. Chem.*, *5*, No. 50.
[6] Kuschel, F., Hartmann, L., Bauer, M., & Weissflog, W. (2014). *Mol. Cryst. Liq. Cryst.*, *588*, 51.
[7] Gleeson, H. (2014). In *Handbook of Liquid Crystals*, Goodby, J. W., Collings, P. J., Kato, T., Tschierske, C., Gleeson, H. & Raynes, P. (Eds.), Vol. 8., Wiley-VCH: Weinheim.
[8] Greubel W., Wolff W. U., & Krüger H. (1973). *Mol. Cryst. Liq. Cryst.*, *12*, 103.

[9] Bauer M., Boeffel C., Kuschel F., & Zaschke H. (2006). *J. Soc. Info. Disp.*, *14*, 1.
[10] Earl, D. J., & Wilson, M. R. (2003). *J. Chem. Phys.*, *119*, 10280.
[11] Eelkema, R., & Feringa, B. L. (2006). *Org. Biomol. Chem.*, *4*, 3729.
[12] Kamberaj, H., Low, R. J., & Neal, M. P. (2005). *Ferroelectrics*, *315*, 183.
[13] Frezza, E., Pieraccini, S., Mazzini, S., Ferrarini, A., & Spada, G. P. (2012). *Beilstein J. Org. Chem.*, *8*, 155.
[14] Clayden, J., Moran, W. J., Edwards, P. J., & LaPlante, S. R. (2009). *Angew. Chem. Int. Ed.*, *48*, 6398.
[15] Deutscher, H.-J., Laaser, B., Dölling, W., & Schubert, H. (1978). *J. prakt. Chem.*, *320*, 191.
[16] Technical data sheet (2008). Merck KGaA.
[17] Kresse, H., König, S., & Demus, D. (1983). *Z. Chem. 23*, 339.
[18] Hauser, A., Rettig, R., Kuschel, F. & Demus, D. (1986). *Wiss. Z. Univ. Halle*, *5*, 72.
[19] Kessler, H. (1970). *Angew. Chem. Int. Ed.*, *9*, 219.
[20] Modarresi-Alam, A. R., Najafi, P., Rostamizadeh, M., Keykha, H., Bijanzadeh, H. R., & Kleinpeter, E. (2007). *J. Org. Chem.*, *72*, 2208.
[21] Shanan-Atidi, H., & Bar-Eli, K. H. (1970). *J. Phys. Chem.*, *74*, 961.
[22] Mannschreck, A., Mattheus, A., & Rissmann, G. (1967). *J. Mol. Spectros.*, *23*, 15.
[23] Havriliak, S., & Negami, S. (1967). *Polymer*, *8*, 161.
[24] Vogel, H. (1921). *Phys. Z.*, *22*, 645; Fulcher, G. S. (1923). *J. Am. Ceram. Soc., 8*, 339; Tammann, G., & Hesse, W. (1926). *Z. Anorg. Allg. Chem., 156*, 245.
[25] Doolittle, A. K. (1951). *J. Appl. Phys.*, *22*, 1471.
[26] Cohen, M. H., & Turnbull, D. (1959). *J. Chem. Phys.*, *31*, 1164.
[27] Rejmer, W., Czuprynski, K., & Drzewinski, W. (2011). *Mol. Cryst. Liq. Cryst.*, *547*, 33.